Effects of Principal Stress Rotation on Resilient Behavior in Rail Track Foundations

P. J. Gräbe[1] and C. R. I. Clayton[2]

Abstract: The design of a railway track substructure requires a realistic understanding of the resilient behavior of the underlying track foundation materials, namely, the subballast and subgrade layers. Currently, the best available method of characterizing the resilient behavior of track foundation materials is through the execution of cyclic triaxial tests, although these do not have the ability to impose principal stress rotation (PSR) on test specimens. A previous paper by the authors demonstrated that PSR increases the rate of permanent strain development. This paper reports on the effects of PSR on the resilient behavior of track foundation materials. Four different reconstituted soils selected to represent typical track foundation materials were subjected to undrained cyclic and torsional shear tests in a hollow-cylinder apparatus. It was established that PSR reduces the resilient modulus of the materials compared with cyclic loading without PSR. The effects of PSR as a function of clay content, overconsolidation ratio (OCR), and consolidation regime (isotropic or anisotropic) were also investigated.

Author keywords: Cyclic loads; Laboratory tests; Shear tests; Railroad tracks; Stress; Resilient modulus.

Introduction

Rail track foundations are subjected to a large number of repeated loads at levels below the shear strength of the material (Brown 1996). A single load of moderate magnitude on a well-designed pavement structure (road or rail) produces predominantly recoverable (resilient) deformations, but repeated loads cause irrecoverable or permanent strains. It is the combination of these that determines the design and long-term performance of a pavement (Li and Selig 1996).

Gräbe and Clayton (2003, 2009) discussed the effects of principal stress rotation (PSR) on permanent deformation behavior in rail track foundations and concluded that PSR has a significant and deleterious impact on permanent deformation of some types of foundation materials. Cyclic triaxial testing, which cannot impose PSR, therefore will not necessarily give good estimates of long-term performance of rail track foundations.

This paper focuses on the effect of PSR on resilient behavior, an equally important aspect when dealing with the design of rail track foundations. Burrow et al. (2007) compared five different railway track foundation design methods from the United States, United Kingdom, Europe, and Japan and found that four parameters principally determine the design thickness, as suggested by the different design procedures. These parameters are subgrade resilient modulus, axle load, speed, and cumulative tonnage.

[1]Professor and Chair in Railway Engineering, Dept. of Civil Engineering, Univ. of Pretoria, Pretoria, Gauteng 0002, South Africa (corresponding author). E-mail: hannes.grabe@up.ac.za

[2]Professor, Dept. of Infrastructure Engineering, Univ. of Southampton, Southampton SO17 1BJ, U.K.; and Extraordinary Professor, Dept. of Civil Engineering, Univ. of Pretoria, Pretoria, Gauteng 0002, South Africa. E-mail: c.clayton@soton.ac.uk

Resilient Deformation Behavior

Resilient behavior and characterization of the resilient modulus of pavement layers can be used as a basis on which to predict pavement behavior under cyclic loads (Hveem 1955; Seed et al. 1962; Hicks and Monismith 1971; O'Reilly and Brown 1991; Li 1994; Brown 1996).

The term *resilient modulus* was first introduced in California following pioneering work at the University of California, Berkeley (Hveem 1955; Hicks and Monismith 1971). The resilient modulus of a soil is the stiffness of the soil calculated from recoverable strains under repeated loading and unloading. The resilient modulus E_r is traditionally calculated from stress and strain values as measured in a triaxial test (Bishop and Henkel 1962) and is equivalent to Young's modulus, hence the choice of the symbol E_r.

$$E_r = \frac{q_r}{\varepsilon_r} \tag{1}$$

where q_r = repeated deviator stress or stress pulse; and ε_r = resilient (recoverable) strain.

The main justification for using elastic theory is that under a single load application, well-designed flexible pavement layers will respond in a largely resilient manner, deformations will be almost entirely recovered when unloading takes place, and any irrecoverable deformations will be small relative to the resilient component. This will be true only if the applied loading is significantly less than the maximum shear strength and once a significant number of load cycles have been applied. It has to be appreciated that for a compacted subgrade, evaluation of the resilient modulus alone does not permit a determination of total pavement deflection or prediction of the fatigue life of the pavement (Brown 1996).

O'Reilly and Brown (1991) justify use of the resilient modulus in pavement design as follows:

> Consider the idealized behavior of elements of dry granular soil subjected to regular drained cycling during stress-controlled loading. Each cycle is accompanied by a change in shear strain, some of which is recoverable and some of which is not. The magnitude of the recoverable strain remains fairly constant

during each cycle. On the other hand, the irrecoverable or plastic strain developed during each successive cycle tends to reduce with increasing number of cycles. Eventually, the soil attains a form of equilibrium for this loading pattern, at which stage the magnitude of the recoverable strain experienced during any cycle greatly exceeds the plastic strain increment for that cycle and the behavior can be described as quasi-elastic or resilient. It is well established that the resilient stiffness of soils is stress level dependent and is also dependent on the magnitude of resilient shear strain.

Resilient behavior is influenced by a number of factors that can be grouped into three categories (Li and Selig 1994; Lekarp et al. 2000).

1. Loading condition or stress state, which includes the magnitude of deviator stress and confining stress, the number of repetitive loadings, their sequence, and stress history;
2. Soil type and structure, which includes aggregate type, particle shape, fines content, and grading and which also depends on the compaction method and compaction effort for a new subgrade; and
3. Soil physical state, which is defined by moisture content, void ratio, and density and which is subject to environmental changes.

Numerous empirical models (e.g., bilinear, power, semilog, hyperbolic, and octahedral) have been developed to relate resilient modulus E_r to the cyclic deviator stress q_r and the initial average effective stress p'_0, as well as the plastic limit w_p, moisture content w, and optimal moisture content w_{opt} (Li and Selig 1994; Lekarp et al. 2000; Brown 1996). Relationships based on a power model are frequently used because of their simplicity and satisfactory ability to model the resilient modulus. Although E_r increases with increasing confining stress, it has been found to have a much less significant effect on E_r than the deviator stress for fine-grained subgrade soils, especially clay soils (Fredlund et al. 1975). For this reason, Li and Selig's (1994) power relationship relates resilient modulus only to the cyclic deviator stress

$$E_r = Kq_r^n \tag{2}$$

where K and n are soil-specific constants that are determined by carrying out repeated-load (cyclic) triaxial tests. For granular pavement materials, the resilient modulus has been related to effective stress by Brown (1975) with the following empirical relationship:

$$E_r = K\left(\frac{p'_0}{q_r}\right)^n \tag{3}$$

where $E_r = 3G_r$ for saturated, undrained conditions; G_r = resilient shear modulus; and p'_0 = initial average effective stress. As before, K and n are soil-specific constants that are determined by carrying out repeated-load (cyclic) triaxial tests that do not involve any PSR or the crossing of the isotropic stress state.

Experimental Work

The research described in this paper is based on hollow-cylinder tests carried out on pairs of specimens to compare the difference in resilient deformation behavior of specimens in which no PSR occurred and of specimens in which PSR was applied. Full details of the apparatus, instrumentation, and materials that were tested can be found in the authors' previous paper that deals with permanent deformation behavior (Gräbe and Clayton 2009). For clarity, these aspects will be mentioned and summarized in the following paragraphs.

Apparatus

The hollow-cylinder apparatus (HCA) that was used in this research (Gräbe 2001) employed two servomotors to control axial and torsional movement, respectively, and had a maximum cycling rate of 2 Hz. The axial force and deformation were applied through the base of the cell, whereas the same actuator imposed both torque and angular rotation. High-accuracy digital controllers were used for the internal and external cell pressures. A closed-loop control algorithm integrated the high-speed data acquisition and the control of all peripheral components. For these tests, the HCA specimens had internal and external diameters of 60 and 100 mm, respectively, and a height of 200 mm.

Instrumentation

A schematic diagram showing a front and plan view of the instrumentation that was developed and used for the HCA tests is provided in Fig. 1. The volume changes of the saturated specimen and of the fluid volume of the inner chamber were measured by a digital pressure-volume controller. A convenient simplification to the stress paths was the equalization of the internal and external cell pressures in all tests, enabling calculation of the radial stress on the specimen as well as other related stress parameters.

An internal submersible load-torque transducer with a 10 kN/30 N·m rating was mounted in the top of cell to measure vertical force and torque. Axial displacement was measured globally (between the top and bottom faces of the test specimen) as well as locally (over the middle third of the specimen). Thus an encoder mounted on the axial actuator motor shaft measured global axial displacement, whereas two linear variable differential transformers (LVDTs) on opposing sides of the specimen measured local axial displacement. A LVDT attached to a radial caliper measured radial displacement of the external diameter of the specimen. As with axial displacement, global and local instrumentation was used to measure angular rotation owing to torsion of the specimen. A radial actuator shaft encoder was used for measuring global angular rotation and shear strain, whereas a specially designed circumferential ring with a LVDT was used to measure angular rotation over the middle third of the specimen (see Fig. 1).

The pore-water pressure in the specimen was measured at the top and base with external silicon diaphragm pressure transducers. In addition to these measurements, a midplane probe was installed at the midheight of the specimen to enable measurement of rapid changes in the pore-water pressure during cyclic loading.

Material Description

Four reconstituted materials (A, B, C, and D) were created to present the range of material found in typical railway foundations. Different size fractions of Leighton Buzzard sand, Oakamoor HPF4 silica flour, and Hymod Prima Ball clay were combined to produce the four materials. Given the size of the hollow-cylinder soil specimens, the maximum particle size of the four materials was restricted to 1.18 mm. The reconstituted materials nevertheless provide a reasonable representation of typical track foundation material (subballast and subgrade material but not the ballast) as found on the South African heavy-haul coal line (Gräbe and Shaw 2010). The composition and characteristics of the materials are shown in Table 1, whereas the particle size distributions of the four reconstituted

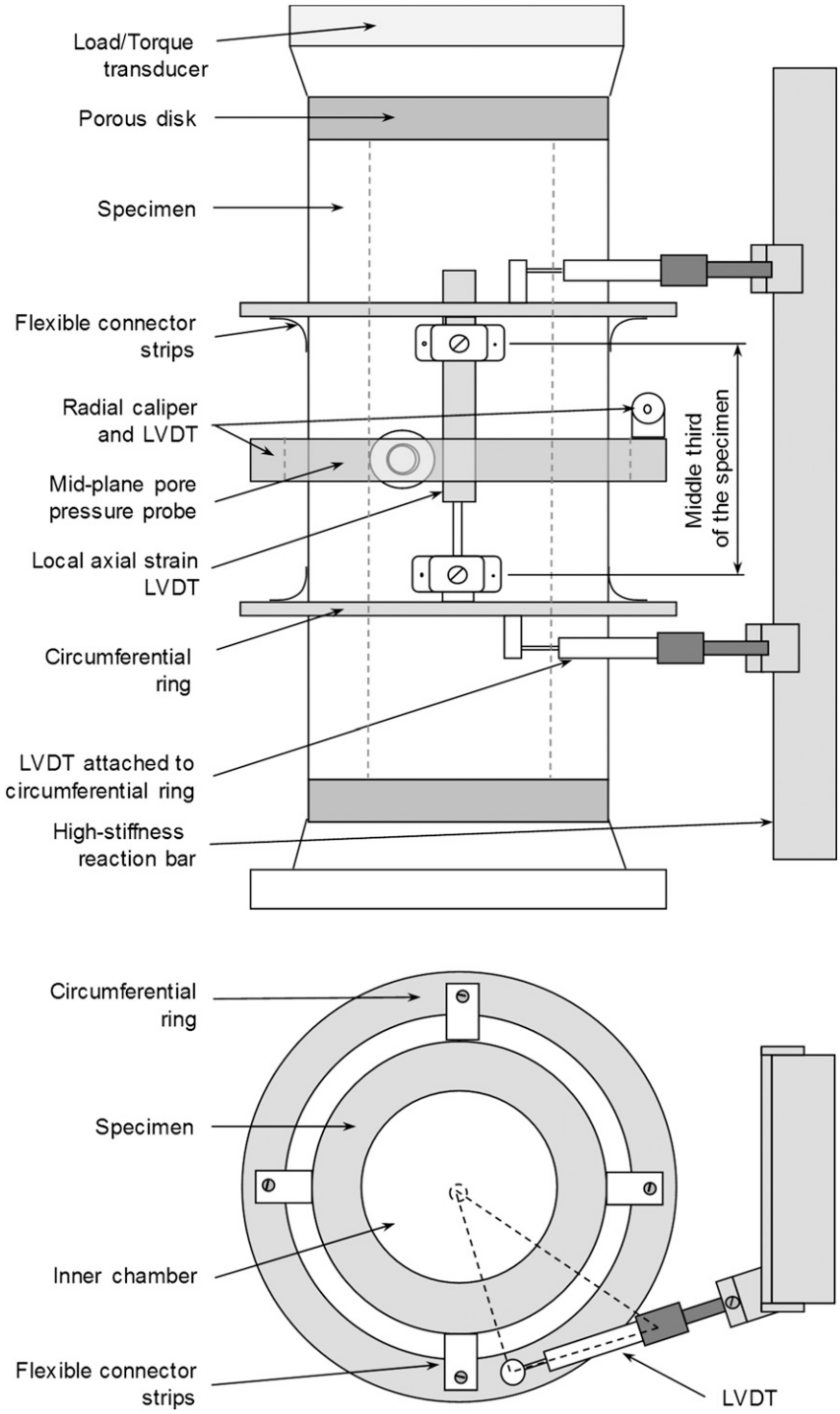

Fig. 1. Instrumentation for measuring stress and strain on HCA specimen (front and plan views)

materials, as well as scanning electron micrographs of the constituent materials, are given by Gräbe and Clayton (2009).

Hollow-Cylinder Testing

Specimen Preparation

All four materials were produced by blending the desired proportions of dry clay, silt, sand, and deaired water in a commercial mixer. The slurry had a moisture content of approximately 45% before the consolidation process commenced. Preconsolidation of the material was done in a centrifuge strongbox subjected to a unidirectional vertical consolidation stress of 200–300 kPa. During preconsolidation, the moisture content of the materials reduced considerably to between 10.0 and 17.3%. After preconsolidaton, the specimens were cut from the batch of material, trimmed to the desired dimensions in a soil lathe, and placed in the HCA. The specimen was enclosed with an outer and inner rubber membrane before installation of the local instrumentation. Following this, most of the specimens were consolidated isotropically to 450 kPa and swollen back to an effective stress of 30 kPa to give an

Table 1. Composition and Characteristics of Reconstituted Materials (Data from Gräbe and Clayton 2009)

Component	Particle size	Reconstituted material A	B	C	D
		Percentages by weight of constituents			
Sand (Leighton Buzzard)	Fraction B 600−1,180 μm	51	47	43	32
	Fraction C 300−600 μm	11	10	9	7
	Fraction D 150−300 μm	11	10	9	7
Silt (HPF4)	5−150 μm	19	21	23	27
Clay (Hymod Prima)	<125 μm	8	13	16	27
		Resulting compositions of mixes (%)			
Sand content		79	73	68	54
Silt content		14	16	18	22
Clay content		7	11	14	24
		Plasticity of mixes			
Plastic limit (percentage)		14	14	14	16
Liquid limit (percentage)		25	28	31	37
Plasticity index (percentage)		11	14	17	21
Activity (A)		1.4	1.3	1.2	0.9
		Critical-state parameters of mixes			
N_o		1.70	1.56	1.45	1.30
$-\lambda$		0.064	0.047	0.035	0.018
$\nu_{\kappa o}$		1.34	1.28	1.24	1.20
$-\kappa$		0.010	0.006	0.003	0.002

overconsolidation ratio (OCR) of 15. This value was chosen based on compaction pressures measured during construction of a railway foundation (Gräbe and Clayton 2009). Two specimens were consolidated to produce an OCR of 25 for investigating the effect of PSR on materials with higher OCR values. Consolidation of the specimens further reduced the moisture content of the materials to between 9.3 and 14.2%. The initial moisture contents of the different specimens (before cyclic loading) were proportional to their clay content.

Stress Paths

The HCA cyclic-stress paths were based on the results of a three-dimensional dynamic finite-element (FE) analysis of a typical heavy-haul track foundation (Gräbe and Clayton 2009). By applying a vertical (σ_z), radial (σ_r), and shear stress ($\tau_{\theta z}$) to a hollow, cylindrical soil sample and cycling these stresses according to the calculated stress paths, the stress paths resulting from repeated train-wheel loading were simulated. The soil specimens were subjected to a cyclic deviator stress of 30 kPa and, in the case of PSR loading, a torsional stress that was cycled between −7 and +7 kPa. The phase difference between the vertical and torsional loadings was one-quarter of the loading period. Fig. 2 shows the calculated (idealized) and applied stress paths for cyclic loading with and without PSR.

After placement in the HCA and completion of all instrumentation, specimens were subjected to the following test stages:

- Backpressure saturation at an effective stress of 30 kPa and maximum cell pressure of 300 kPa. The pore-pressure coefficient B was found to be 0.98 and higher in all cases, indicating that the specimens were saturated.
- Isotropic consolidation with equal internal and external cell pressures to a mean effective stress of 450 kPa.
- Swelling back to an effective stress of 30 kPa, resulting in an OCR of 15.
- HCA cyclic triaxial and torsion shear tests to simulate train loading and to investigate the effect of PSR on the resilient deformation behavior of the railroad-track foundation materials. All tests described in this paper were performed undrained on saturated specimens, therefore preventing volume change and allowing the development of excess pore-water pressures during their final test stage.

In addition to the tests just described, this study also included a limited number of tests to investigate the effect of anisotropy and the degree of overconsolidation on the deformation behavior of one of the materials, namely, Material C (14% clay). Fig. 3 shows the isotropic and anisotropic consolidation and swelling paths that were followed for these tests.

Results and Discussion

It was stated that resilient deformation behavior is influenced by loading condition or stress state, soil type, structure, and soil physical state (Li and Selig 1994; Lekarp et al. 2000). The stress state and stress history of the samples were intentionally kept constant, with the exception of PSR, which was introduced as the primary influencing factor.

Pairs of samples were tested and compared. For each material, a test without PSR (i.e., Specimens A1, B1, C1, and D1) was performed, followed by a second test on another identical specimen but this time with the addition of PSR (i.e., Specimens A2, B2, C2, and D2). For the investigation of anisotropy and the degree of overconsolidation, specimen pairs C3 and C4 and C5 and C6 were tested in a similar way.

A total of 1,000 cycles were performed on each test specimen, except for Specimen A2, which failed after 300 cycles. In the following paragraphs, the resilient deformation behavior of these pairs of specimens will be discussed and compared with the study of the effect of PSR.

Pore Pressure Response

It was found that there was very slight change in the pore pressure during cyclic loading without PSR for all four materials. This change was at most ±2 kPa. When PSR was introduced, Material C (14% clay) and Material D (24% clay) also showed insignificant change in the pore pressure during cyclic loading. However, Material A (7% clay) developed an excess pore pressure of approximately 13 kPa after 300 cycles and subsequently failed. Material B (11% clay) showed a slight increase of 3 kPa in its pore pressure development during cyclic loading with PSR.

Resilient Deformation

Resilient deformation was assessed by plotting the hysteresis loops for the last 10 cycles of the 1,000 cycles carried out on the four materials both for the cyclic triaxial tests and for the cyclic torsional shear tests. For the purpose of this comparison, the axial-strain datum ($\varepsilon_a = 0\%$) of the hysteresis loops was taken as the point at which the loading leg of the cycles started. Fig. 4 shows the deviator stress q versus axial strain ε_a plots where the hysteresis loops with and without PSR are compared. It should be noted that the last 10 cycles before failure are displayed for Specimen A2.

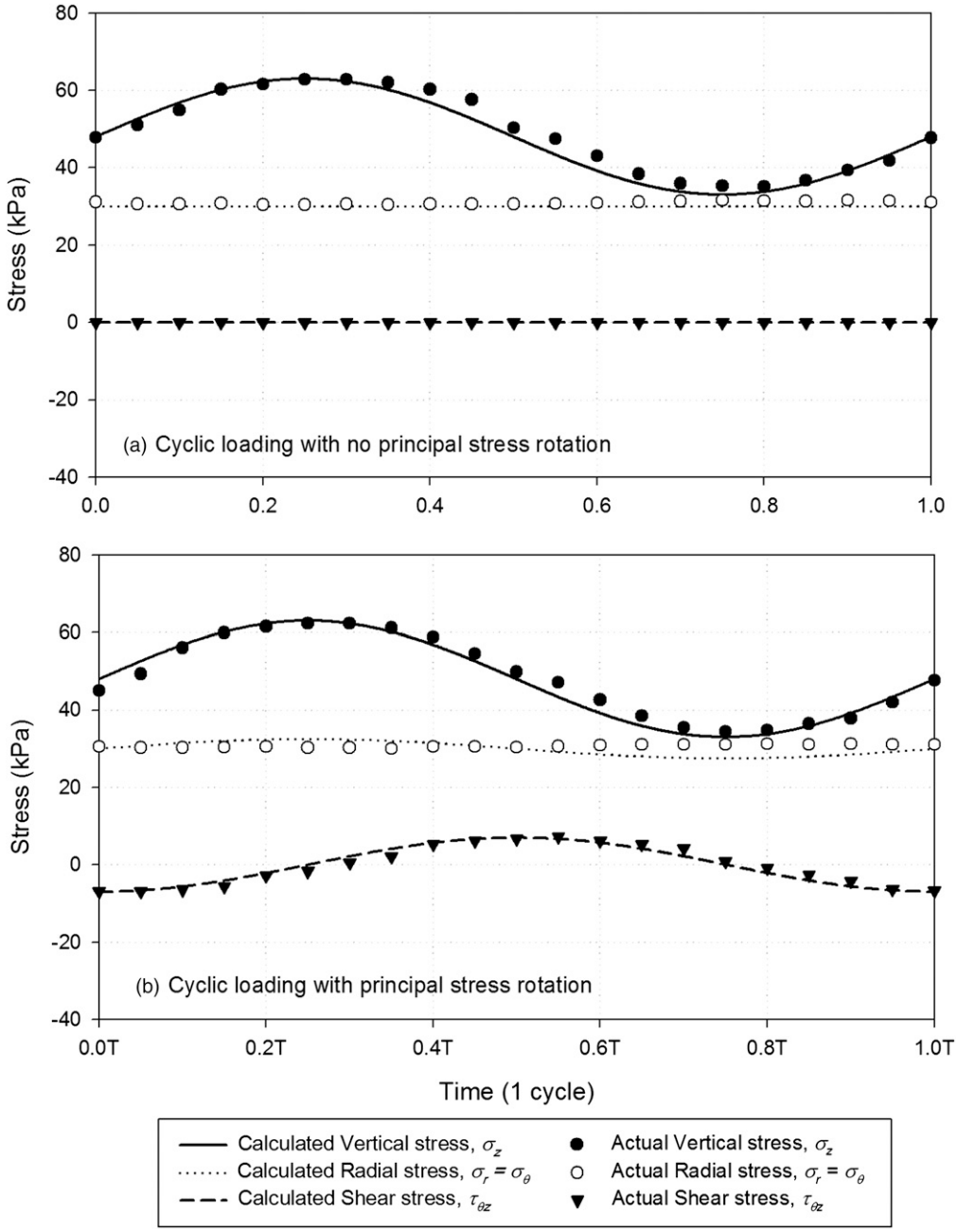

Fig. 2. Calculated (idealized) and actual HCA stress paths in terms of applied stresses for cyclic loading with and without PSR ($K_0 = 1$) (Gräbe and Clayton 2009, © ASCE)

A study of the graphs reveals at least two differences between the tests with and without PSR. First, the hysteretic effect (or damping) of the cyclic measurements becomes more pronounced when PSR is introduced. The slope of the hysteresis loops, representing Young's modulus of the material, is lower with PSR compared with the same slope when the material is loaded without PSR. The graph also shows how the shapes of the hysteresis loops changed as the clay content of the samples increased. This trend is further demonstrated in Fig. 5, where hysteretic damping was calculated and plotted according to the method proposed by Hardin and Drnevich (1972). The higher the clay content, the more hysteretic the behavior became. With the exception of the 7% clay specimen that failed prematurely, hysteretic damping also increased with clay content as a result of PSR.

Resilient Moduli

Because of the hysteretic stress-strain relationship during cyclic loading, the E_r values were based on calculation of an equivalent resilient Young's modulus E_{eq} after Shibuya et al. (1992). The formula for E_{eq} calculates the slope of the stress-strain relationship during a full unload-reload cycle as opposed to other modulus parameters such as E_{sec}, E_{tan}, and E_{max} that consider the secant, tangential, and maximum values of the slope of the stress-strain relationship.

Fig. 6 shows the calculated E_{eq} values for the undrained cyclic loading of Materials A (7% clay), B (11% clay), C (14% clay), and D (24% clay), respectively. Two series of values are presented on the graph, namely, E_{eq} values for cyclic loading without PSR

(Specimens A1, B1, C1, and D1) and those for cyclic loading with PSR (Specimens A2, B2, C2, and D2).

All the materials showed significant strain hardening during the initial 10–20 cycles, after which the change in the resilient modulus per log cycle became approximately constant, i.e., plotting linearly on a logarithmic scale. In all cases, a lower resilient modulus was observed for the samples in which the principal stresses were rotated in comparison with the samples in which no PSR occurred.

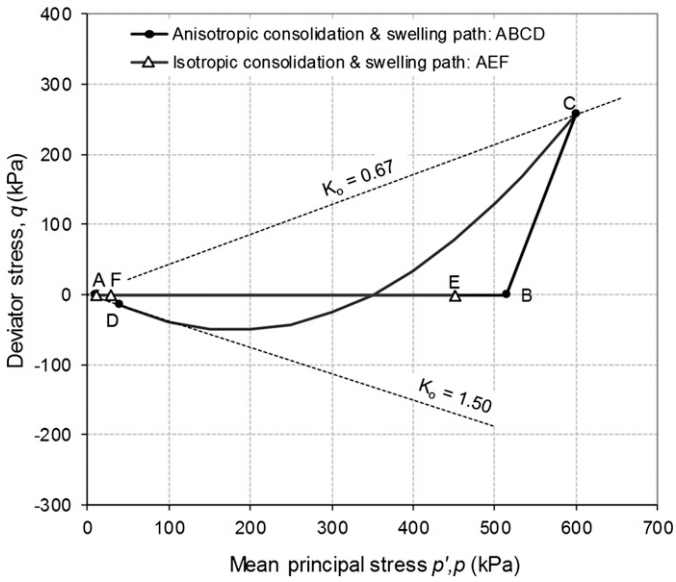

Fig. 3. Isotropic and anisotropic consolidation and swelling stress paths

To quantify the degree to which PSR affected the resilient behavior of the different materials, the following relationship was defined:

$$\mathrm{PSR_{res}} = \frac{E_{eq,\overline{1,000}}}{E_{eq,\overline{1,000}}} \tag{4}$$

where $\mathrm{PSR_{res}}$ = ratio defining the effect of PSR on resilient behavior; $E_{eq,\overline{1,000}}$ = average E_{eq} of 1,000 cycles of cyclic loading without PSR; and $E_{eq,\overline{1,000}}$ = average E_{eq} of 1,000 cycles of cyclic loading with PSR.

Table 2 gives a summary of the calculated E_{eq} values, the resilient strains ε_r for a cyclic deviator stress σ_d of 30 kPa, and the $\mathrm{PSR_{res}}$ values that were calculated for Materials A, B, C, and D. The E_{eq} values ranged from 31 to 90 MPa.

These values are relatively low compared with typical moduli required in track design, which are achieved by compacting unsaturated materials using heavy vibratory rollers where unsaturated conditions prevail and dynamic compaction is used. For example, in South Africa, values ranging from 70 to 500 MPa were measured during field monitoring for compacted selected subgrade and subballast layers (Gräbe et al. 2005).

Fig. 7 illustrates the relationship between the E_{eq} values and the clay content of the different specimens. In all cases, lower E_{eq} values were obtained for specimens that were subjected to PSR compared with those without PSR. Initially, for the isotropically consolidated OCR = 15 samples with clay contents ranging from 7 to 14%, the resilient moduli values increased, followed by a sudden decrease in

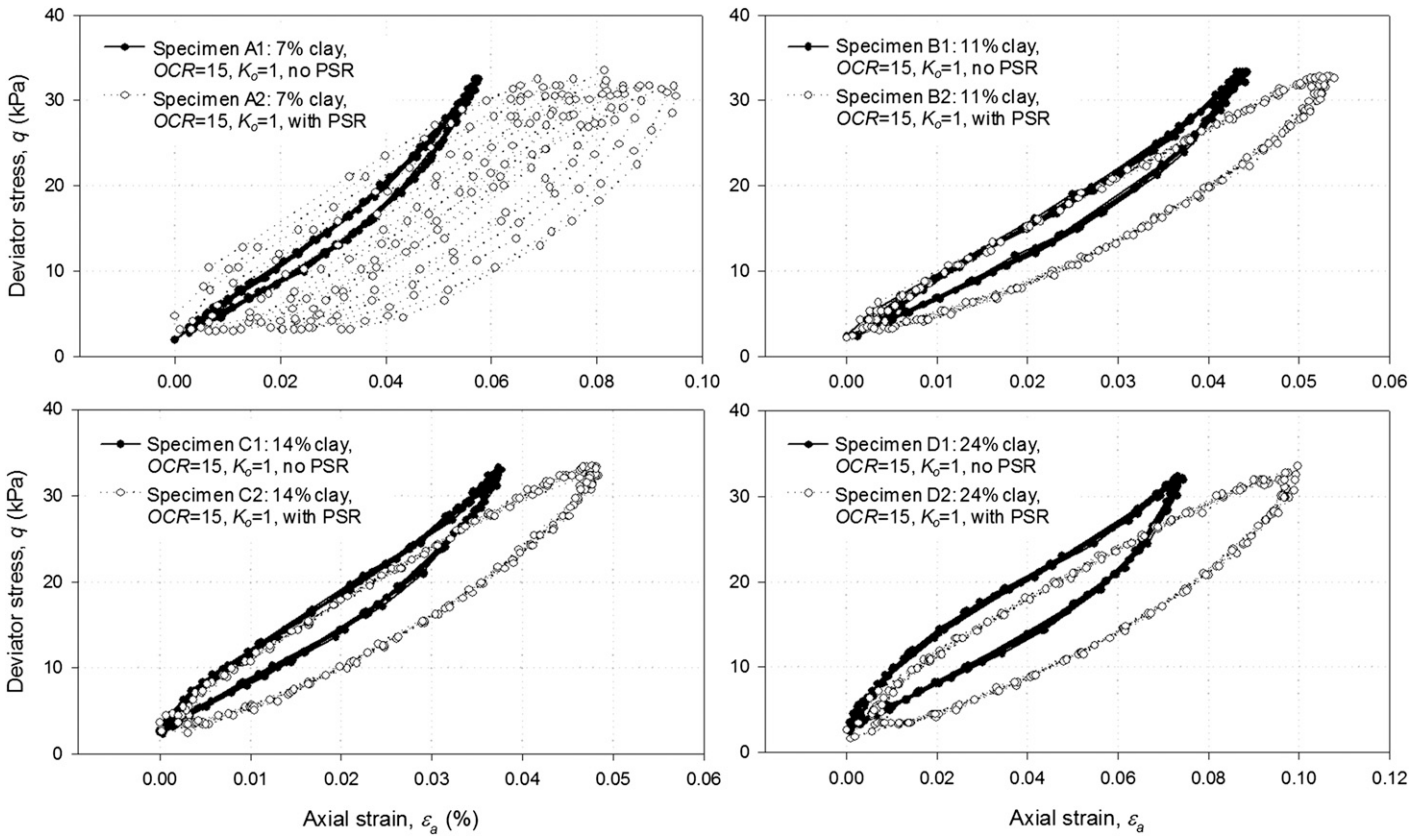

Fig. 4. Hysteresis loops of last 10 of 1,000 cycles: Materials A, B, C, and D (the last 10 of ~300 cycles in the case of Specimen A2)

modulus at 24% clay. The reason for this behavior is related to the fact that at low clay content (7–14%), coarse-grain-to-coarse-grain contact is prevalent, and the clay adds to the stiffness through void filling. However, once the clay prevents coarse-grain-to-coarse-grain contact (at >14% clay), the behavior of the material is essentially that of a clay, in which the coarse grains act merely as a filler within the clay, resulting in reduced stiffness.

For a constant clay content of 14%, higher E_{eq} values were obtained from the specimens with the higher OCR values, as expected. On the other hand, anisotropic consolidation produced specimens with lower E_{eq} values compared with the isotropically consolidated specimens for the same clay content and OCR (see Fig. 7).

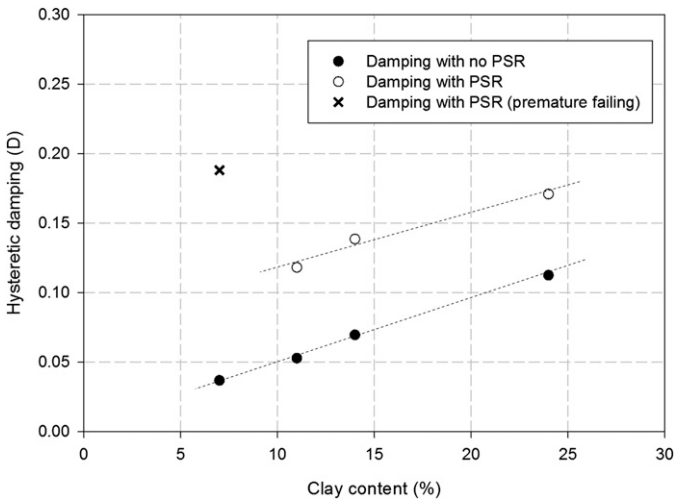

Fig. 5. Hysteretic damping as a function of clay content and principal-stress rotation

Fig. 8 shows the relationship between the calculated equivalent resilient modulus ratios with and without PSR (PSR_{res} values) and the clay contents of the different specimens. The degree to which PSR affected the resilient behavior of the materials decreased with an increase in clay content (when the OCR and consolidation regime remain unchanged). However, even for the most clayey material (Material D with 24% clay), PSR produced a reduction of approximately 22% in the observed resilient modulus of the material. The moisture content of the samples before cyclic loading was proportional to the clay content, and it therefore also could be argued that the degree to which PSR affects resilient behavior depends on the moisture content of the soil specimen; i.e., the lower the moisture content, the higher is the effect of PSR.

The effect of PSR was less for material that was subjected to anisotropic consolidation compared with material consolidated isotropically (comparing the results from Specimens C3 and C4). Similarly, the results of Specimens C5 and C6, consolidated with an OCR of 25 compared with the OCR of 15 used for the rest of the specimens, also indicate that PSR has a lesser effect on materials with higher OCR values.

Other researchers (Chan and Brown 1994; Thom and Dawson 1996) have performed cyclic loading without PSR and cyclic loading with PSR directly after each other on the same specimen. Although it was decided to perform these two different types of cyclic-stress paths on separate but identical samples so that both samples would have been subjected to the same stress history before the start of the cyclic loading, the alternative approach was also

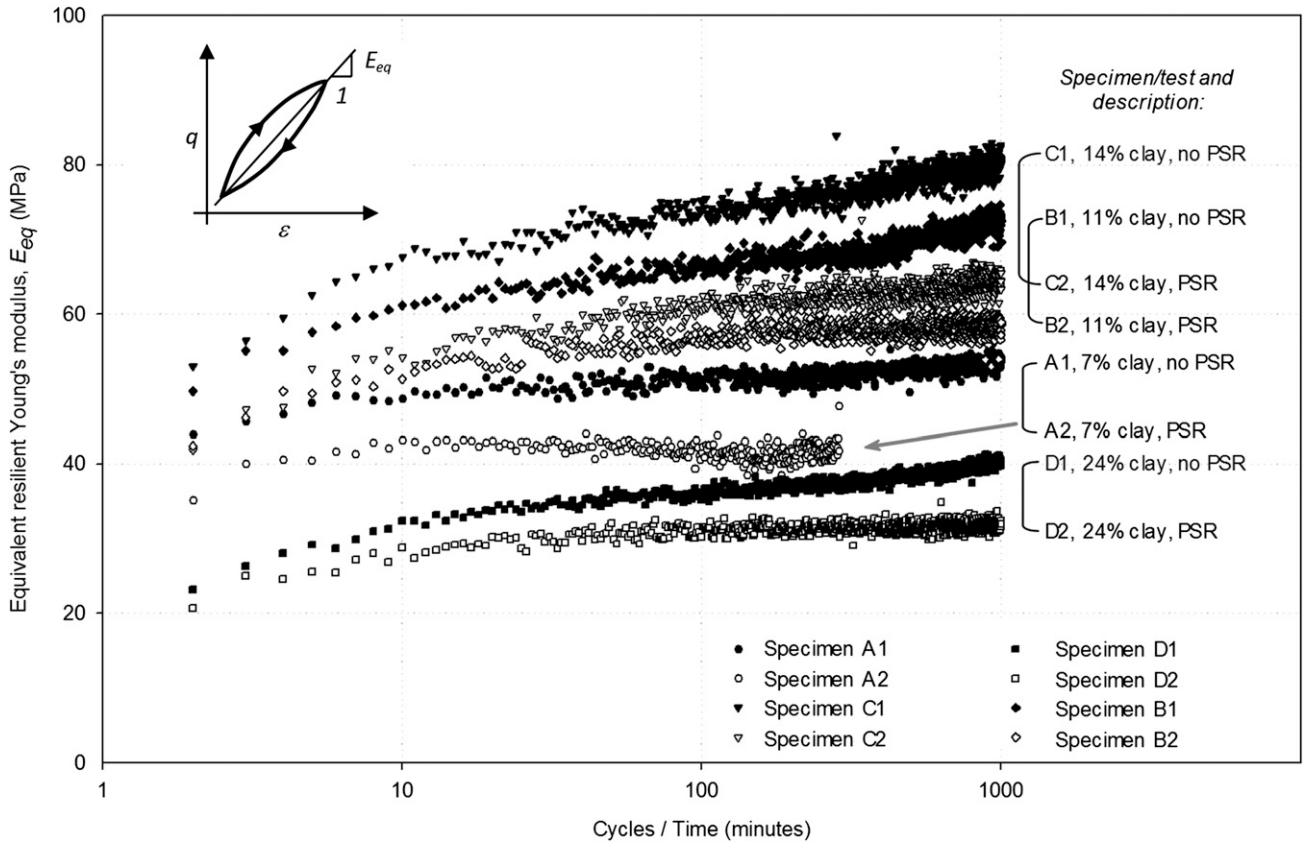

Fig. 6. Resilient modulus during 1,000 loading cycles: Materials A, B, C, and D (OCR = 15; $K_0 = 1$; $\sigma_d = 30$ kPa)

Table 2. Measured Resilient Deformation Parameters

Specimen	Sample preparation	Test description	$E_{eq,1,000}$ (MPa)	ε_r(%)	PSR_{res}
A1 (7% clay)	Isotropic consolidation, OCR = 15, $K_0 = 1$	Cyclic compression with no PSR	53	0.057	1.260
A2 (7% clay)	Isotropic consolidation, OCR = 15, $K_0 = 1$	Cyclic compression with PSR	42	0.071	
B1 (11% clay)	Isotropic consolidation, OCR = 15, $K_0 = 1$	Cyclic compression with no PSR	72	0.042	1.233
B2 (11% clay)	Isotropic consolidation, OCR = 15, $K_0 = 1$	Cyclic compression with PSR	58	0.052	
C1 (14% clay)	Isotropic consolidation, OCR = 15, $K_0 = 1$	Cyclic compression with no PSR	78	0.038	1.233
C2 (14% clay)	Isotropic consolidation, OCR = 15, $K_0 = 1$	Cyclic compression with PSR	63	0.048	
C3 (14% clay)	Anisotropic consolidation, OCR = 15, $K_0 = 1$	Cyclic compression with no PSR	69	0.043	1.218
C4 (14% clay)	Anisotropic consolidation, OCR = 15, $K_0 = 1$	Cyclic compression with PSR	57	0.053	
C5 (14% clay)	Isotropic consolidation, OCR = 25, $K_0 = 1$	Cyclic compression with no PSR	90	0.033	1.200
C6 (14% clay)	Isotropic consolidation, OCR = 25, $K_0 = 1$	Cyclic compression with PSR	75	0.040	
D1 (24% clay)	Isotropic consolidation, OCR = 15, $K_0 = 1$	Cyclic compression with no PSR	38	0.079	1.215
D2 (24% clay)	Isotropic consolidation, OCR = 15, $K_0 = 1$	Cyclic compression with PSR	31	0.097	

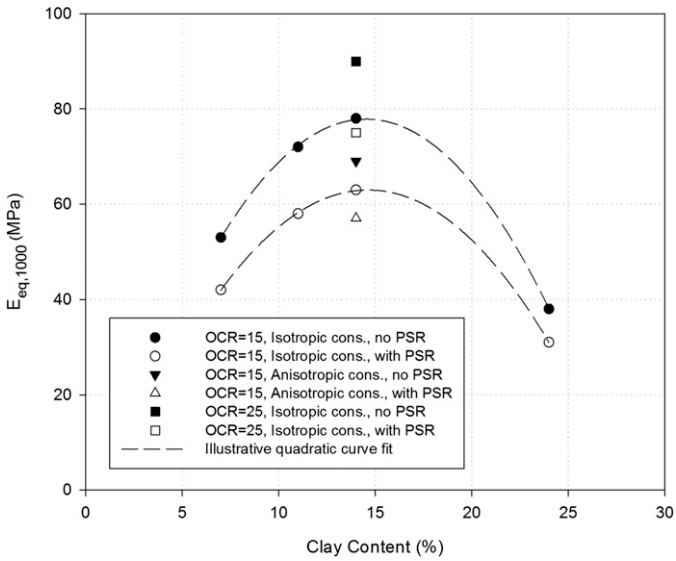

Fig. 7. Average equivalent resilient modulus after 1,000 cycles as a function of clay content for different OCR values and consolidation regimes

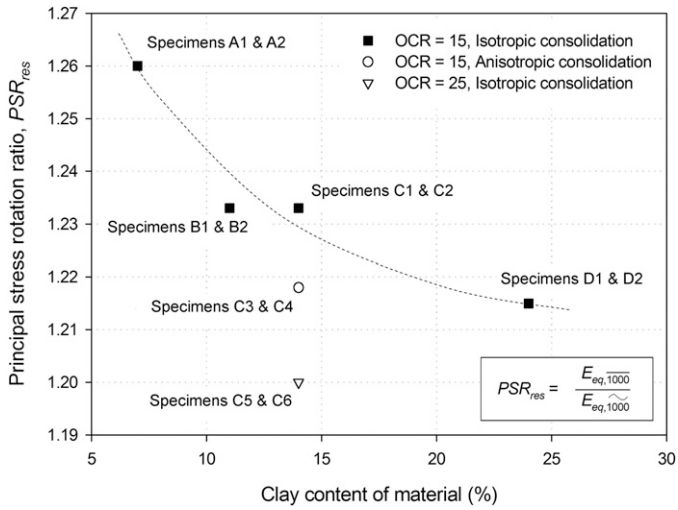

Fig. 8. Effect of PSR on resilient behavior (based on E_{eq}) as a function of clay content

investigated. This was done by carrying out a second phase of the cyclic testing, i.e., another 1,000 loading cycles following the initial 1,000 cycles, but this time with PSR for the samples that were subjected to axial loading only and with no PSR for the samples that were subjected to axial and torsional loading. In this way, the effect of stress history on the resilient behavior could be investigated.

Figs. 9 and 10 show the change in E_{eq} during 2,000 cycles of axial and torsional loading on Materials C (14% clay) and D (24% clay), respectively. Although the two figures present series of E_{eq} values that have different ranges for the different materials, the behavior of both follows the same basic trend. When observing the axial and torsional loading (with PSR) phases, it is clear that the E_{eq} values (after a rapid initial increase) remain more or less constant during the remainder of the 1,000 cycles regardless of whether it forms part of the first of second phases of cyclic loading. In contrast, the E_{eq} values of the axial-loading cycles (no PSR) show a constant increase with logarithm of applied cycles after an initial rapid increase.

When PSR is introduced following 1,000 cycles without PSR, a sudden drop in the E_{eq} values is observed. The opposite occurs when PSR is removed following 1,000 cycles with PSR, i.e., a sudden increase in resilient modulus. Depending on the order of the cyclic loading or stress history, the materials tested ended with significantly different resilient moduli. In both cases, the difference in final E_{eq} value was approximately 12 MPa.

Conclusions

In this study, pairs of samples were subjected to undrained cyclic loading in a HCA. Four different materials, typically found in railway foundations and with clay contents ranging from 7 to 24%, were tested under cyclic triaxial and torsional shear conditions. One of the two identical samples was subjected to cyclic loading with no PSR, whereas the second sample was subjected to cyclic loading with PSR.

In a previous paper (Gräbe and Clayton 2009) it was concluded that PSR has the effect of increasing the rate of permanent strain of the four materials compared with standard cyclic triaxial tests, which cannot apply PSR. The extent of this effect was indirectly proportional to the clay content of the specimens that were tested.

This paper has focused on the effect of PSR on the resilient behavior of the same materials. It was found that PSR also has a significant effect on the equivalent resilient moduli E_{eq} that were calculated for the cyclic-loading tests. PSR reduced the resilient moduli of the specimens by approximately 20–26% depending on

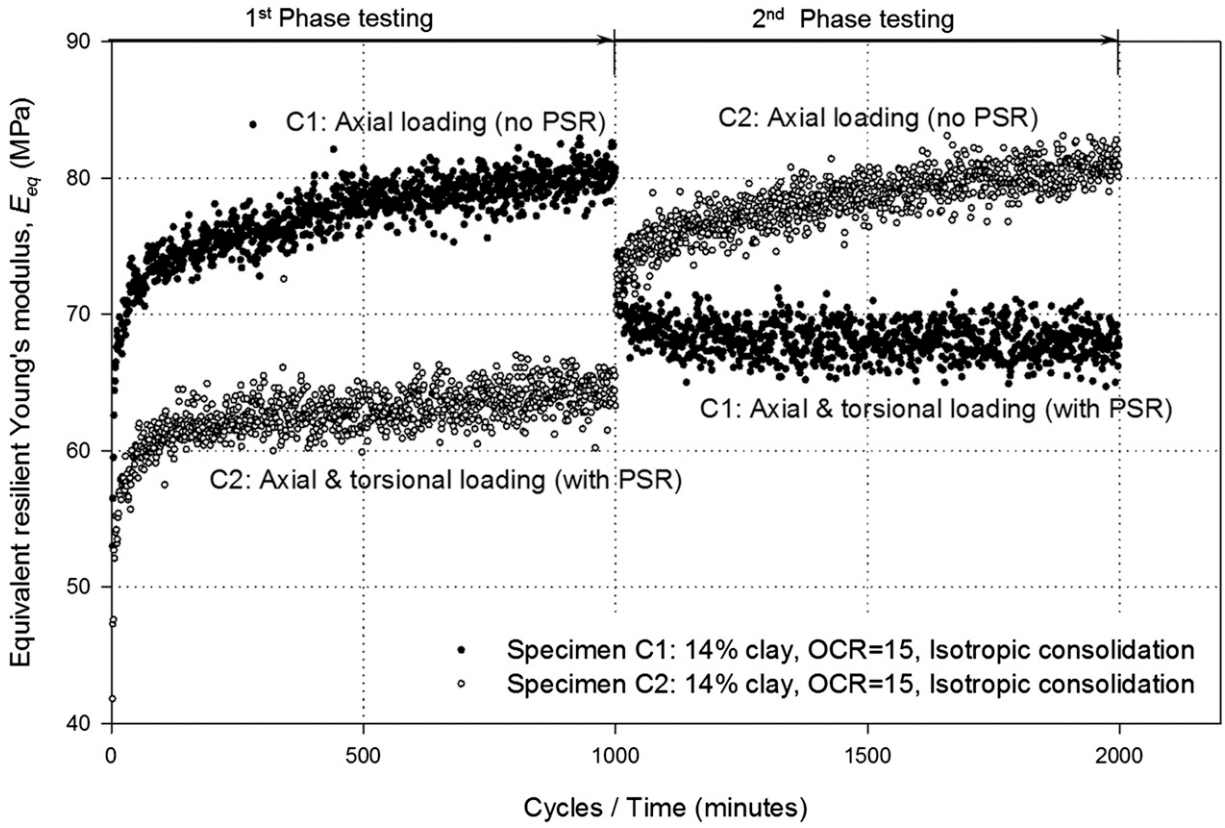

Fig. 9. Effect of stress history and PSR on resilient behavior: Material C (14% clay; OCR = 15; $K_0 = 1$; isotropic consolidation)

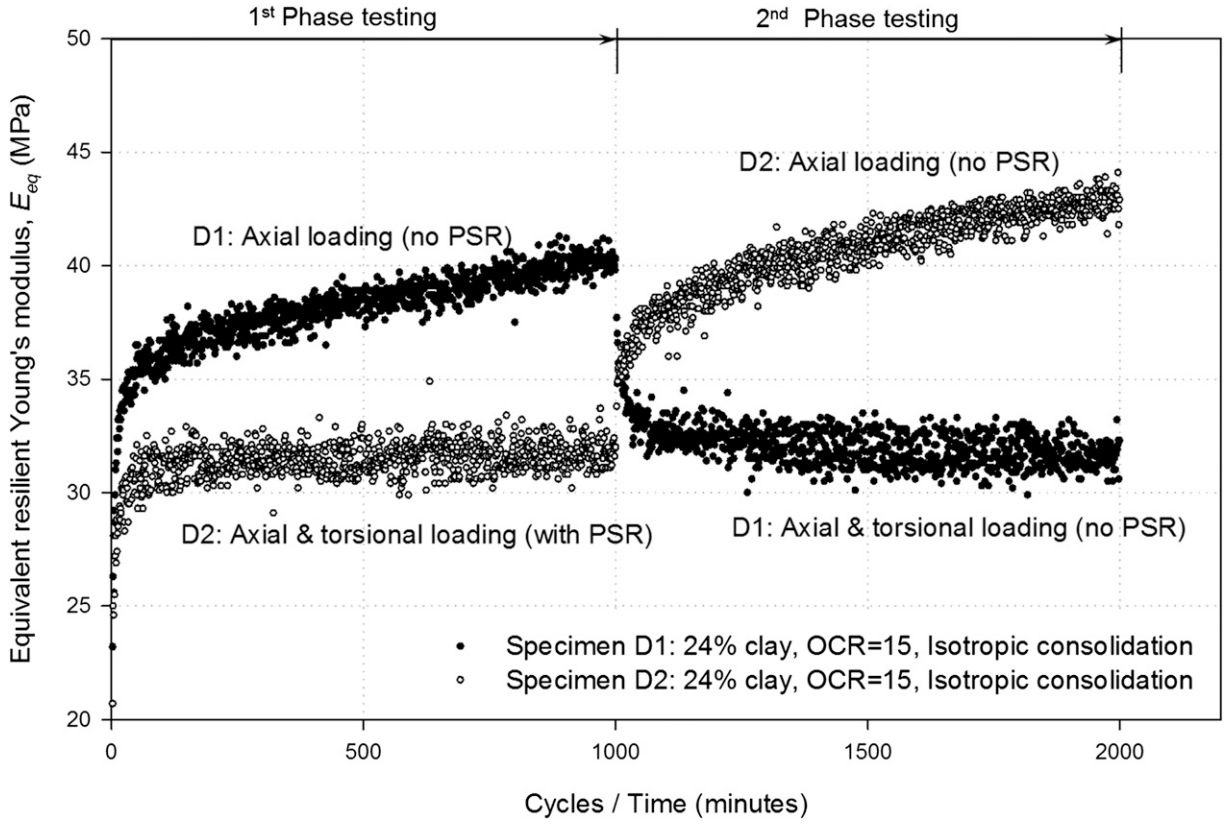

Fig. 10. Effect of stress history and PSR on resilient behavior: Material D (24% clay; OCR = 15; $K_0 = 1$; isotropic consolidation)

the OCR, clay content, and consolidation regime followed in preparation of the specimen. The clay content of the materials determined the moisture content before cyclic loading. Materials with lower clay content and consequently also lower moisture content (with OCR = 15 and isotropic consolidation) were more susceptible to the effect of PSR.

In material with a clay content of 14%, a higher OCR of 25 resulted in a reduction in the effect of PSR on the resilient modulus. Similarly, anisotropic consolidation of the material also resulted in a reduction in the effect of PSR on the resilient modulus compared with the isotropically consolidated specimens.

A mainly linear relationship was also observed between the hysteretic damping D and the clay content of the tested materials, with D being proportional to the clay content. In addition, PSR resulted in a further increase in D for a given clay content.

Principal stress rotation, caused by moving wheel loads in road and rail transportation systems, therefore reduces the resilient moduli of foundation materials. The degree to which PSR influences resilient modulus was shown to depend on the stress state (i.e., OCR, consolidation regime, and stress history), soil type (i.e., clay content as an aspect of grading), and soil physical state (i.e., moisture content). However, all tested materials (with varying clay contents) were susceptible to the effects of PSR given undrained cyclic train loading.

The track engineer should consider this phenomenon, especially when using foundation moduli obtained from cyclic triaxial tests, because these cannot rotate the principal stresses. In practice, the complexity of HCA testing might limit the usefulness of this testing methodology, in which case the designer should use the PSR_{res} values to adjust (i.e., reduce) the resilient moduli obtained from triaxial testing to account for the effect of PSR. The long-term behavior of track foundations also should be analyzed in light of the possible decreases in modulus because they may reduce the design life of the track structure.

References

Bishop, A. W., and Henkel, D. J. (1962). *The measurement of soil properties in the triaxial test*, Edward Arnold, London.

Brown, S. F. (1975). "Improved framework for predicting permanent deformation in asphalt layers." *Transportation Research Record 537*, Transportation Research Board, Washington, DC, 18–30.

Brown, S. F. (1996). "Soil mechanics in pavement engineering." *Geotechnique*, 46(3), 383–426.

Burrow, M. P. N., Bowness, D., and Ghataora, G. S. (2007). "A comparison of railway track foundation design methods." *Proc. Inst. Mech. Eng. F: J. Rail Rapid Transit*, 221(1), 1–12.

Chan, F. W. K., and Brown, S. F. (1994). "Significance of principal stress rotation in pavements." *Proc., 13th Int. Conf. on Soil Mechanics and Foundation Engineering*, International Society of Soil Mechanics and Geotechnical Engineering, London, 1823–1826.

Fredlund, D. G., Bergan, A. T., and Sauer, E. K. (1975). "Deformation characterisation of subgrade soils for highways and runways in northern environments." *Can. Geotech. J.*, 12(2), 213–223.

Gräbe, P. J. (2001). "Resilient and permanent deformation of railway foundations under principal stress rotation." Ph.D. thesis, Univ. of Southampton, Southampton, U.K.

Gräbe, P. J., and Clayton, C. R. I. (2003). "Permanent deformation of railway foundations under heavy axle loading." *Proc., Int. Heavy Haul Association (IHHA)*, IHHA, Virginia Beach, VA, 3.25–3.32.

Gräbe, P. J., and Clayton, C. R. I. (2009). "Effects of principal stress rotation on permanent deformation in rail track foundations." *J. Geotech. Geoenviron. Eng.*, 10.1061/(ASCE)1090-0241(2009)135:4(555), 555–565.

Gräbe, P. J., and Shaw, F. J. (2010). "Design life prediction of a heavy haul track foundation." *Proc. Int. Mech. Eng. F: J. Rail Rapid Transit*, 224(5), 337–344.

Gräbe, P. J., Shaw, F. J., and Clayton, C. R. I. (2005). "Deformation measurement on a heavy haul track formation." *Proc., 8th Int. Heavy Haul Conf.*, IHHA, Virginia Beach, VA, 287–295.

Hardin, B. O., and Drnevich, V. P. (1972). "Shear modulus and damping in soils." *J. Soil Mech. and Found. Div.*, 98(7), 667–692.

Hicks, R. G., and Monismith, C. L. (1971). "Factors influencing the resilient response of granular materials." *Highway Research Record 345*, Highway Research Board, National Academy of Sciences, Washington, DC, 15–31.

Hveem, F. N. (1955). "Pavement deflections and fatigue failures." *Highway Research Board Bulletin 114*, Highway Research Board, National Academy of Sciences, Washington, DC, 43–87.

Lekarp, F., Isacsson, U., and Dawson, A. R. (2000). "State of the art. I: Resilient response of unbound aggregates." *J. Transp. Eng.*, 10.1061/(ASCE)0733-947X(2000)126:1(66), 66–75.

Li, D. (1994). "Railway track granular layer thickness design based on subgrade performance under repeated loading." Ph.D. thesis, Univ. of Massachusetts, Amherst, MA.

Li, D., and Selig, E. T. (1994). "Resilient modulus for fine-grained subgrade soils." *J. Geotech. Engrg.*, 10.1061/(ASCE)0733-9410(1994)120:6(939), 939–957.

Li, D., and Selig, E. T. (1996). "Cumulative plastic deformation for fine-grained subgrade soil." *J. Geotech. Engrg.*, 10.1061/(ASCE)0733-9410(1996)122:12(1006), 1006–1013.

O'Reilly, M. P., and Brown, S. F. (1991). *Cyclic loading of soils: From theory to design*, Blackie, Glasgow, U.K., 1–18.

Seed, H. B., Chan, C. K., and Lee, C. E. (1962). "Resilience characteristics of subgrade soils and their relation to fatigue failures." *Proc., Int. Conf. on the Structural Design of Asphalt Pavements*, ASCE, Reston, VA, 611–636.

Shibuya, S., et al. (1992). "Elastic deformation properties of geomaterials." *Soils Found.*, 32(3), 26–46.

Thom, N. H., and Dawson, A. R. (1996). "The permanent deformation of a granular material modelled using hollow cylinder testing." *Proc., European Symp. Euroflex: Flexible Pavements*, A. Gomes Correia, ed., Taylor & Francis, London, 97–119.